Cortical processing of global form, motion and biological motion under low light levels

Eliza Burton [a,*], John Wattam-Bell [b,1], Gary S. Rubin [a], Janette Atkinson [b,c], Oliver Braddick [c], Marko Nardini [d,a,*]

[a] Institute of Ophthalmology, University College London, London, UK
[b] Division of Psychology and Language Sciences, University College London, London, UK
[c] Experimental Psychology, University of Oxford, UK
[d] Department of Psychology, Durham University, Durham, UK

ABSTRACT

Advances in potential treatments for rod and cone dystrophies have increased the need to understand the contributions of rods and cones to higher-level cortical vision. We measured form, motion and biological motion coherence thresholds and EEG steady-state visual evoked potentials (SSVEP) responses under light conditions ranging from photopic to scotopic. Low light increased thresholds for all three kinds of stimuli; however, global form thresholds were relatively more impaired than those for global motion or biological motion. SSVEP responses to coherent global form and motion were reduced in low light, and motion responses showed a shift in topography from the midline to more lateral locations. Contrast sensitivity measures confirmed that basic visual processing was also affected by low light. However, comparison with contrast sensitivity function (CSF) reductions achieved by optical blur indicated that these were insufficient to explain the pattern of results, although the temporal properties of the rod system may also play a role. Overall, mid-level processing in extra-striate areas is differentially affected by light level, in ways that cannot be explained in terms of low-level spatiotemporal sensitivity. A topographical shift in scotopic motion SSVEP responses may reflect either changes to inhibitory feedback mechanisms between V1 and extra-striate regions or a reduction of input to the visual cortex. These results provide insight into how higher-level cortical vision is normally organised in absence of cone input, and provide a basis for comparison with patients with cone dystrophies, before and after treatments aiming to restore cone function.

© 2016 Published by Elsevier Ltd.

1. Introduction

The current study investigates the impact of low light conditions on global motion, biological motion, and, for the first time, global (static) form perception. This was achieved using a combination of behavioural psychophysics and steady-state visual evoked potentials (SSVEP) under light intensities ranging from photopic to scotopic levels.

The study aimed to understand the contribution of rods and cones to global form, global motion and biological motion perception. These measures have become increasingly used as indicators of visual function beyond early processing in primary visual cortex. With the advance of new treatments for rod and cone dystrophies, such as gene therapy (Bainbridge et al., 2015; Cideciyan et al., 2008; Jacobson et al., 2012; Komáromy et al., 2010; Sundaram et al., 2014; Zelinger et al., 2015) it is becoming increasingly important to understand how different aspects of visual function, including higher cortical visual functions, are influenced by rod and cone loss. Gaining an understanding of visual function in observers with healthy vision under light conditions designed to activate rods and/or cones will provide important baseline information for comparison with retinal dystrophy patients before and after treatment with new therapies.

Form perception is known to be predominantly processed in ventral stream areas such as V4 (Gallant, Shoup, & Mazer, 2000; Ostwald, Lam, Li, & Kourtzi, 2008; Wilkinson et al., 2000), whilst motion perception is dominated by dorsal stream areas such as MT/V5 and MST (Braddick et al., 2001; Harvey, Braddick, &

* Corresponding author at: Department of Psychology, Durham University, Durham, UK (M. Nardini).

E-mail addresses: eliza.burton@ucl.ac.uk (E. Burton), marko.nardini@durham.ac.uk (M. Nardini).

[1] Deceased 30.12.2013.

Cowey, 2010; Rees, Friston, & Koch, 2000). This functional segregation allows for differences in the development and potential vulnerabilities of the two pathways to be explored and as a result global form and motion perception have been studied extensively in both typically developing (Atkinson et al., 2004; Braddick, Atkinson, & Wattam-Bell, 2003; Golarai, 2009; Gunn et al., 2002) and atypical populations (Atkinson et al., 1997; Ellemberg, Lewis, Maurer, Brar, & Brent, 2002; Kogan et al., 2004; Lewis et al., 2002; Taylor, Jakobson, Maurer, & Lewis, 2009). The present research, leading up to work with patient populations who developed with atypical visual input, will also allow us to better understand the development of global form, global motion and biological motion perception.

Previous research into visual perception under low light has generally studied early-level visual processing including detection of local motion, visual acuity, stereopsis, flicker fusion and spectral sensitivity (Barlow, 1962; Cavonius & Robbins, 1973; Kellnhofer, Ritschel, Vangorp, Myszkowski, & Seidel, 2014; Kinney, 1958; Livingstone & Hubel, 1994; Mandelbaum & Sloan, 1947; Nygaard & Frumkes, 1985; Riggs, 1965; Teller, 2009; Westheimer, 1965). Research exists into reading under scotopic conditions (Chaparro & Young, 1989, 1993), however research into mid- and high-level vision is relatively sparse.

Whilst our study is primarily concerned with the impact of scotopic and mesopic conditions on mid- and high-level vision, it is also important to consider how far these effects may result from the impact of these conditions on the processing of lower-level mechanisms. Area V1 performs local processing of visual signals, which go on to be integrated for global form and motion processing. Duffy and Hubel (2007) looked at basic receptive field properties of V1 neurons in macaques, including directional selectivity and orientation selectivity, and found that these were maintained in scotopic conditions. This has implications for both global motion and form perception as it suggests that at the local level, perception should be unimpaired. However, other properties of scotopic vision may impact on early visual perception which in turn may affect global processing. For example, visual acuity is known to be reduced in scotopic conditions due to the poor spatial resolution of the rod system. Maximum scotopic acuity is ∼0.7 LogMAR as opposed to −0.2 LogMAR in photopic conditions (Riggs, 1965). Reduced acuity may lead to reduced sensitivity to local cues necessary for later integration into global constructs. We have investigated elsewhere (Burton et al., 2015) the effects of reduced acuity and contrast sensitivity on global form and motion processing. Scotopic vision also has relatively sluggish temporal properties, at least in central areas of the visual field, which may have an impact on motion processing (Conner, 1982; Takeuchi & De Valois, 2000).

Studies into coherent motion perception under low light have found it to be generally preserved (Billino, Bremmer, & Gegenfurtner, 2008; Grossman & Blake, 1999). Grossman and Blake (1999) examined coherent motion thresholds under low light using random dot kinematograms (RDK). Translational coherent motion moving at 3.2 deg/s was presented to participants in a 2-interval forced choice task under photopic and scotopic conditions and participants were required to indicate the presence of coherent motion. They reported that coherence thresholds were the same under low light as photopic conditions. Billino et al. (2008) tested detection of translational coherent motion under three light intensities using RDKs. They found that detection thresholds became progressively worse as luminance fell from 98.5 to 0.285 and 0.018 cd/m².

Biological motion perception was also investigated in these two studies. Billino et al. (2008), asked participants to detect intact or phase-scrambled biological motion under the three light levels mentioned previously. The motion was embedded within random noise dots and on each trial the proportion of noise dots (i.e. dots' signal to noise ratio) was varied to establish participants' perceptual threshold. Performance revealed a U-shaped result with best performance in photopic conditions, worst performance at mesopic light levels (0.285 cd/m²) and scotopic performance, at 0.018 cd/m², falling between the two. In contrast, Grossman and Blake (1999) found biological motion detection to deteriorate in low light. However, they only tested under the two light levels 3.6 and 0.036 cd/m². Testing in darker conditions might have resulted in the U-shaped performance described by Billino et al. (2008).

SSVEPs have not previously been used to study scotopic form and motion perception. However, they have been used in the study of global form and motion development (Hou, Gilmore, Pettet, & Norcia, 2009; Norcia et al., 2005; Palomares, Pettet, Vildavski, Hou, & Norcia, 2009; Wattam-Bell et al., 2010; Weinstein et al., 2012). For example, Wattam-Bell et al. (2010) found distinct difference between infant and adult global form and motion SSVEP topographies. It remains unclear how much these differences reflect immaturities in extra-striate regions, or are a result of lower-level limitations of spatial vision in infancy. Testing under low light conditions will therefore also provide further insight into how global form and motion topography is affected when spatial visual input is reduced.

The current study aimed to build on and extend previous research into visual perception in low light. The light conditions extended over a wider range than those previously used (Billino et al., 2008; Grossman & Blake, 1999) to test vision well into the scotopic range. To obtain a fuller picture of extra-striate processing, we tested perception of coherent form as well as of coherent motion and biological motion. As well as behavioural tests of sensitivity, steady-state EEG measures were used to investigate changes in the amplitudes and cortical distributions of neural responses underlying global form, global motion and biological motion perception under different light levels.

2. Material and methods

2.1. General

2.1.1. Participants

Twenty normally sighted participants (mean age 25.2 years, standard deviation 4.6) completed the experiment within the Faculty of Brain Sciences, Division of Psychology and Language Sciences, University College London. Informed consent was obtained before testing commenced. All work was carried out in accordance with the Code of Ethics of the World Medical Association (Declaration of Helsinki) and experiments were approved by the UCL ethics committee.

2.1.2. Light levels

Four light levels were used in the experiment. This was done in order to assess the relative contribution of rods and cones to perceptual sensitivity and cortical EEG responses. Light levels were achieved using sheets of characterised neutral density filters (Sabre International Ltd, UK) which were placed over the display monitor. There was no other light source in the room besides the display screen.

The four luminance levels were classified as photopic (8.7 cd/m²), high mesopic (0.8 cd/m²), low mesopic (2.7×10^{-2} cd/m²) and scotopic (8.7×10^{-4} cd/m²). The values here refer to the luminance of the dots/lines making up the stimuli; these were presented against a black background with a 3.24 Log Weber Contrast (LogWC) for each light level. Behavioural tests were completed under the four light conditions whilst EEG tests were

Table 1
Mean and standard deviation of retinal illuminance level (log STr) for each light level, for the sample of participants whose pupil sizes were measured.

	Mean (SD) retinal illuminance, log STr
Photopic	3.21, (0.08)
High mesopic	1.71, (0.08)
Low mesopic	0.30, (0.08)
Scotopic	−1.15, (0.06)

completed under the high mesopic and scotopic conditions. Testing at all four light levels for the EEG would have required a lengthy test period which would have impacted on the quality of the data. The high mesopic and scotopic conditions were selected in order to provide an informative spread of luminance levels.

Participants were dark adapted prior to testing (see Section 2.4 for further details). However, tests were completed with a natural pupil so that the precise retinal illuminance for each condition varied between participants. To address how large this variation was and to check that retinal illuminance fell within photopic, mesopic and scotopic conditions, a subset of participants ($N = 5$) had their retinal illuminance levels calculated, based on their pupil size under each condition. Pupil size was measured by taking an image of the pupil whilst viewing the form stimuli at 60 cm. Images were captured with an infrared camera and pupil diameter was calculated using image processing software. At retinal illuminance levels above 3 log scotopic trolands (log STr), rods become saturated and cones take over, whilst the mesopic range is defined as falling between −1 and 2 log STr (Stockman & Sharpe, 2006). Mean illuminance levels are shown in Table 1, confirming that on average participants were viewing the stimuli in the desired luminance ranges and that individual pupillary variations were minor.

2.1.3. Stimuli generation and task design

All stimuli were generated using a PC in Matlab (MATLAB, 2012) using the Psychophysics Toolbox extensions (Brainard, 1997; Kleiner et al., 2007; Pelli, 1997) and displayed on a Mitsubishi Diamond Pro SB2070 22″ CRT monitor with a 60 Hz refresh rate. Participants completed tests at a viewing distance of 60 cm, at which the monitor display subtended 37° × 28°.

2.2. Behavioural measures

2.2.1. Coherent form and motion

Coherent form and motion stimuli consisted of 2000 white dots, each with a 6 pixel diameter and 0.29° visual angle, plotted against a black background. To create the form stimuli, multiple dots were plotted forming stationary short arc segments with an average length of 0.58°. The starting locations of line segments were randomly distributed across the display area for each trial. To create the motion stimuli 8 dots were plotted in successive frames creating motion along an arc trajectory at 8.6 deg/s, with a lifetime of 133 ms. In each case, coherently plotted elements were arranged in a circular structure with a common centre of curvature. This produced a region of concentric structure subtending 16°. Outside this region, the arcs were randomly oriented.

The task employed a two-alternative forced-choice (2AFC) design in which coherent form or motion was displayed on one side of the screen, centred 10° from the screen centre. The participant's task was to judge which side contained coherent form or motion. Trials varied in their level of coherence by varying the ratio of coherent to random elements within the circular target region. Participants were asked to fixate on a white central cross whilst
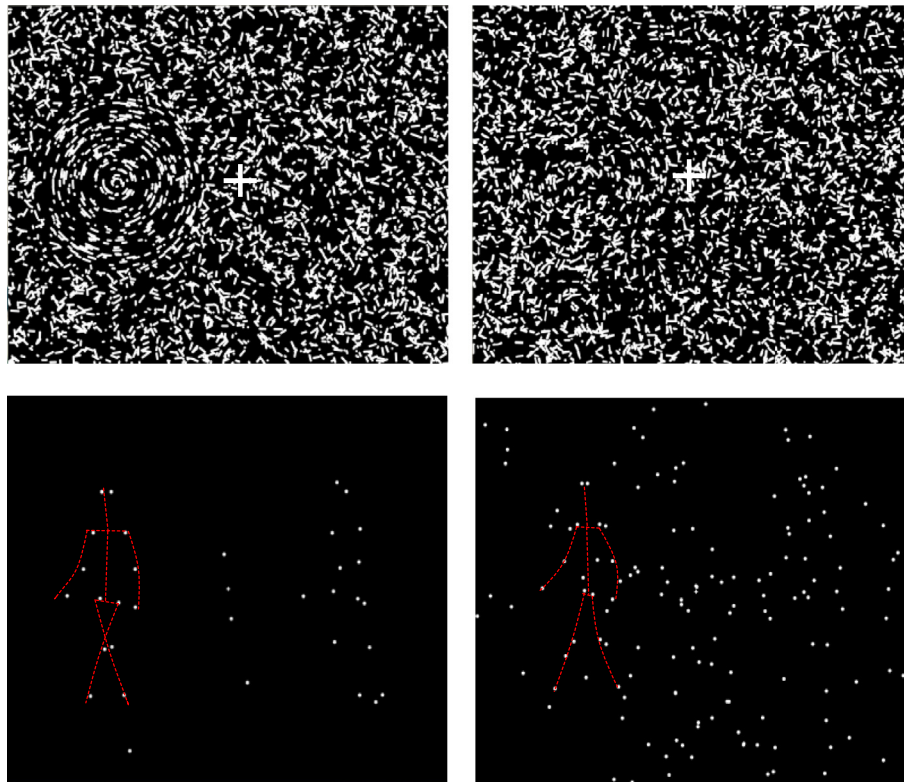

Fig. 1. Example of stimuli from the form and motion task (top) and biological motion task (bottom). Form stimuli are shown here. In the motion task each line segment represents the motion trajectory of a single dot. The left image shows 100% coherence whilst the right image shows 12.5% coherence. The biological motion stimulus is shown with low noise (left) and high noise (right). Red dotted lines are added here to show the location of the biological motion but were not present in the experiment. (For interpretation of the references to colour in this figure legend, the reader is referred to the web version of this article.)

stimuli were presented, at random, on the left or right of fixation as shown in Fig. 1.

Stimuli were presented for 1 s after which time a black screen appeared. The participant then had as much time as they wanted to indicate the location of the target using either a right- or left-hand button.

Participants viewed a total of 90 form and 90 motion trials per light level (3 runs of 30 trials at each). A coherence threshold was calculated from each run, and then averaged across the three runs. On each trial, coherence (% of coherent elements within the target region) was varied according to the PSI adaptive method (Kontsevich & Tyler, 1999) which estimated the threshold as the 75% point on the psychometric function.

2.2.2. Biological motion

Biological motion stimuli were generated using Cutting's Algorithm (Cutting, 1978). Stimuli consisted of point-light figures made up of 14 white dots each with a visual angle of 0.27°. Figures walked on the spot as if on a treadmill and filled an area subtending 15.2° × 5.7°. In order to minimise habituation, the walking figure was rotated about the vertical from trial to trial.

Stimuli were presented alongside a scrambled version of the figure (see Fig. 1). Scrambling was achieved by randomising the starting position of the dots and the phase of the joint angles. The figure was presented from one of five possible angles; straight on, to the left, to the right, diagonally left and diagonally right. The angle was matched on each trial between the biological and scrambled figure. Participants were instructed to indicate the side of the display containing the unscrambled biological motion.

As with the form and motion stimuli, participants viewed 90 trials per light level (3 runs of 30 trials, estimated threshold averaged across the runs). Figures were embedded within random noise dots as shown in Fig. 1. The signal to noise ratio (i.e. proportion of noise dots) on each trial varied based on the PSI adaptive method and the 75% threshold was estimated.

2.2.3. Contrast sensitivity test

In addition to the form, motion and biological motion tests, all participants had their contrast sensitivity function (CSF) measured using the quick CSF (qCSF) method (Lesmes, Lu, Baek, & Albright, 2010). Participants completed a 2AFC test indicating whether they detected a Gabor patch 10° to the left or right of fixation. The Gabor had a Gaussian envelope with standard deviation set to a constant 6°. The Gabor varied in both spatial frequency and contrast from trial to trial. The qCSF test uses a Bayesian adaptive procedure to estimate four parameters of a participants' CSF. These are then used to fit the CSF. Participants viewed 100 trials per light level. The aim of the contrast sensitivity test was to assess the extent to which early-level spatial vision, a prerequisite for processing coherent form and motion, might lead to limitations in low light.

2.3. EEG measures

2.3.1. Coherent form and motion

SSVEP measures were used to index cortical activity related to coherent form and motion processing. Stimuli were matched in design to those used in the behavioural tests, containing 2000 white dots, each with a 6 pixel diameter (0.29° visual angle), plotted against a black background. Unlike in the behavioural stimuli however, these were displayed centrally and filled the entire display (37° × 28°), with no active task required. Participants instead passively viewed the form or motion stimuli. These stimuli have been used and described in previous research (Wattam-Bell et al., 2010).

The display alternated between 100% coherence and 0% coherence at a rate of 4 reversals/s. In the coherent phase, the line seg-

ments or dots aligned to create a circular form or rotational motion respectively. In the incoherent phase, line segments or dots were orientated randomly within the display.

Participants were instructed to remain as still as possible during the EEG recording. A yellow fixation dot was present in the centre of the display throughout the experiment and participants were instructed to fixate this.

2.3.2. Biological motion

Biological motion SSVEPs were attempted but no significant responses were recorded. Only form and motion SSVEP results are therefore discussed here.

2.3.3. SSVEP recording

Recordings were made using a 128-electrode HydroCel Geodesic Sensor Net v.1.0 (Electrical Geodesics Inc., Eugene, Oregon) using the vertex as the reference. Impedance was measured at 20 Hz and individual electrodes were adjusted so that impedance fell below 50 kΩ.

Stimuli were presented in one run of 20 blocks per test (form, motion), per light condition (mesopic, scotopic). Each block included 20 cycles (40 reversals) lasting 10 s. This gave a total of 400 cycles of form and motion stimuli per light condition.

2.3.4. SSVEP analysis

SSVEP signals were digitized at 250 samples per second and a low pass filter was applied (20 Hz, 12 dB/octave). Channels were excluded if their standard deviation exceeded 800 μV and the remaining channels were re-referenced to an average reference. SSVEP data was divided into 500 ms epochs (one stimulus cycle), excluding any epochs with a total voltage excursion greater than 200 μV which was considered an artefact. Channels containing fewer than 30 artefact-free epochs were discarded. The pre-processing procedure was based on standard SSVEP practice (Odom et al., 2010; Picton et al., 2000).

2.3.5. F1 and F2

Fourier analysis was used to extract SSVEP amplitudes and phases at the fundamental frequency (F1 = 2 Hz form/motion) and the second harmonic (F2 = 4 Hz form/motion). The presence of a significant response at each harmonic was tested with the T^2_{circ} statistic (Victor & Mast, 1991) in both first-level (individual) and second-level (group) analyses, as described in Wattam-Bell et al. (2010). This statistic is designed specifically for analysing SSVEPs, and provides a measure of the signal to noise ratio, taking into account the phase and amplitude of the signal at each harmonic.

The fundamental frequency (F1) represents responses at the same frequency as the stimulus cycle. A significant F1 therefore represents activation in response to the onset of global structure of the stimuli, with an asymmetric response to coherence onset vs offset.

A significant F2 represents responses to changes in the stimulus configuration brought on by every stimulus switch. F2 therefore includes responses to local changes in the stimulus configuration. Neural responses to global changes may also be present in F2, however only F1 isolates a signal arising from global changes.

2.4. Experimental design and procedure

Testing was completed in a dark environment with no stray light. All windows and light sources were sealed during the experiment using black-out curtains and tape.

Participants were dark adapted before the tests. For the photopic condition participants were seated in a dim room for

Table 2
The 4 condition orders that were used for behavioural tests.

	Condition				Participants
Order 1	Photopic	High mesopic	Low mesopic	Scotopic	N = 5
Order 2	High mesopic	Low mesopic	Scotopic	Photopic	N = 5
Order 3	Photopic	Scotopic	Low mesopic	High mesopic	N = 5
Order 4	Scotopic	Low mesopic	High mesopic	Photopic	N = 5

10 min before testing began, whilst for the two mesopic and the scotopic conditions participants were given blackout goggles (MindFold, Inc) to wear for 30 min. Light levels were counterbalanced so that half of participants completed the mesopic level, followed by scotopic, whilst half completed the scotopic level followed by mesopic. The photopic level was always completed either at the beginning or end of testing (see Table 2).

Participants began with a practice session, which included all behavioural tests, completed in the photopic light level. The practice involved three runs of the form, motion and biological motion tests, with each run containing 30 trials. Participants also completed one run of the contrast sensitivity test which contained 100 trials. Thresholds across the form, motion and biological motion tests were compared to assess the consistency of each participant's performance. This comparison showed that most participants (18 out of 20) maintained consistent thresholds after three runs. Those who did not do so were given two more runs of the test after which their thresholds were found to be consistent.

For the main experiment, participants completed three runs each of the form, motion and biological tests in each light condition. Each run contained 30 trials. Participants also completed one run of the contrast sensitivity test in each light condition, containing 100 trials. SSVEP testing was carried out after the behavioural tests at the high mesopic and scotopic light levels.

3. Results

3.1. Behavioural

3.1.1. Form, motion and biological motion

Thresholds were averaged across three runs per participant and then across the 20 participants. Group averages for each test and light level can be seen in Fig. 2.

As Fig. 2 shows, performance on all tests showed a progressive worsening as luminance decreased. Thresholds remained stable
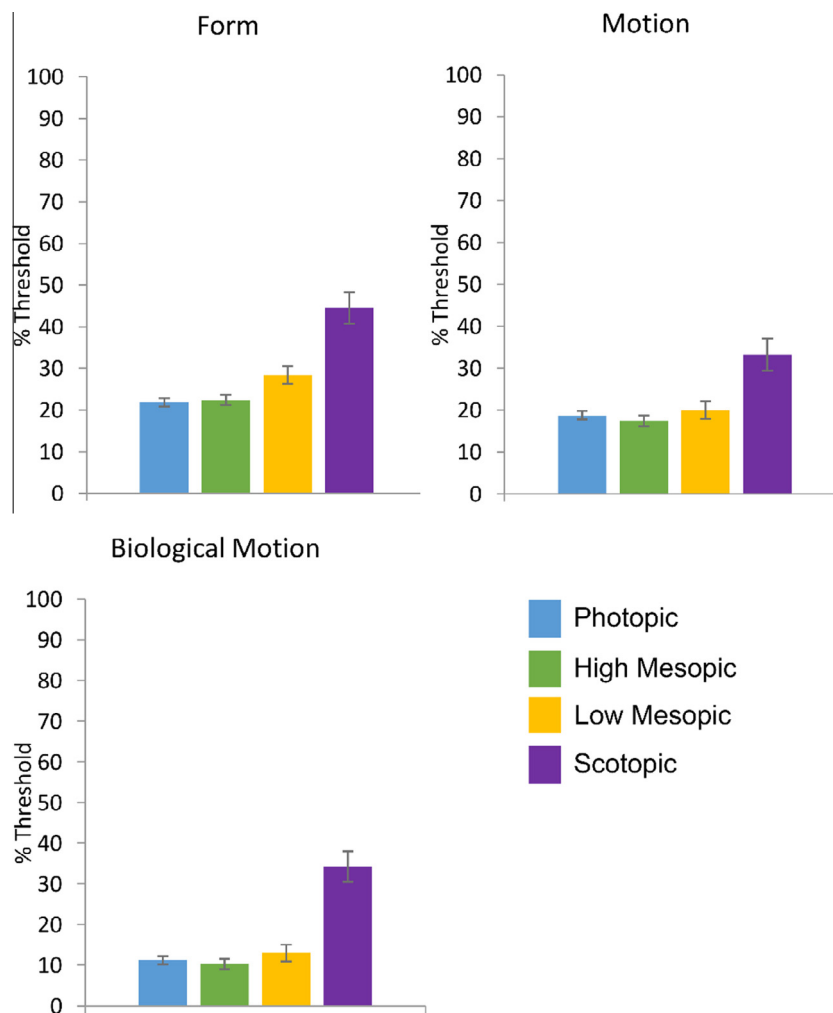

Fig. 2. Mean thresholds for form, motion and biological motion tests under 4 light levels. Error bars represent the standard error of the mean.
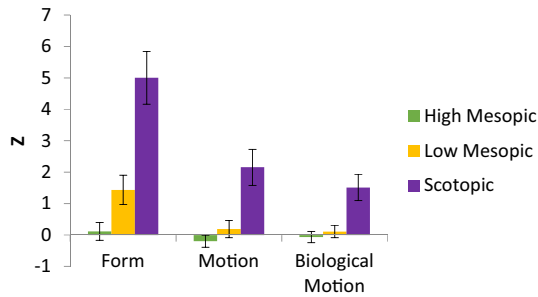
Fig. 3. Mean z-scores for form, motion and biological motion thresholds. Positive z-scores represent higher coherence thresholds and therefore worse test performance. Error bars represent the standard error of the mean.

across the photopic and high mesopic ranges. However, performance on all three tests began to decline in the low mesopic range, leading to a sharp decline in the scotopic range, between 0.027 and 0.00087 cd/m^2.

Repeated-measures ANOVAs revealed main effects of light level on all three tests (form: $F(3,57) = 35.793$, $p < 0.001$; motion: $F(3,57) = 23.272$, $p < 0.001$; biological motion: $F(3,57) = 16.038$, $p = 0.001$).

In order to compare the tests to one another, z-scores with respect to photopic performance were calculated. Participants had their form, motion and biological motion z-scores calculated for each luminance condition in respect to the group average and standard deviation of the photopic condition. These normalised the results so that 0 represents the photopic result for all three tests. Mean z-score results from across participants are shown in Fig. 3 and demonstrate greater impairment with decreasing luminance for coherent form thresholds than for coherent motion or biological motion. A repeated measures ANOVA of the z-scores found a significant main effect of both luminance ($F(2,38) = 42.908$, $p < 0.001$) and test ($F(2,38) = 15.999$, $p < 0.001$) as well as a significant interaction between the two ($F(4,76) = 16.238$, $p < 0.001$). Post hoc comparisons using Bonferroni corrections revealed that the main effect of test type was driven by differences between the form result (mean = 2.187, sd = 2.11) and the other two tests (motion: mean = 0.719, sd = 1.47, biological motion: mean = 0.521, sd = 1.02).

3.2. EEG

3.2.1. SSVEP topography

Fig. 4 shows topographic plots of group-level T^2_{circ} values (a statistical measure of signal-to-noise ratio) for the F1 and F2 responses to form and motion. The plots are thresholded at $p = 0.05$ corrected for false discovery rate (Benjamini & Hochberg, 1995), with non-significant values plotted in green.

In the mesopic condition, motion F1 responses showed peak activation over the occipital midline, whilst the form stimulus produced a lateral F1 response, predominantly in the left hemisphere. This pattern is consistent with previous findings with these stimuli at photopic levels (Wattam-Bell et al., 2010).

The scotopic condition shows a reduced F1 T^2_{circ} value for form but not for the motion response. Form activation remained lateral, albeit reduced, however motion activation showed a shift from an occipital midline response to a lateral response.

At the scotopic light level, F2 responses, which reflect local processing, were localised to the occipital midline for form and motion. Motion F2 responses were reduced to an overall non-significant level.

Whilst T^2_{circ} provides an excellent statistical measure of signal to noise ratio, its dependence on background noise level, which is affected by trial numbers and recording time, can make it hard to compare across different experimental setups. Therefore, form and motion raw amplitudes were also calculated at F1 and F2. These are presented in Fig. S1 in the Supplementary data and show a broad agreement in the patterns of activation shown by the T^2_{circ} measure.

To compare the F1 topographies, the posterior electrodes were divided into five distinct regions, as described in Wattam-Bell et al. (2010), and our signal-to-noise measure (T^2_{circ}) was averaged across the 8 electrodes within each region. This gave 5 mean T^2_{circ} values for form and motion. Fig. 5 shows mean signal-to-noise (T^2_{circ}) across these five regions in mesopic and scotopic conditions. Form responses reduced in the scotopic condition but showed a broadly similar pattern of response across the five regions. Motion responses remained consistently strong in scotopic compared to mesopic conditions, but the pattern of activation changed from a central response mesopically to a more lateral response scotopically.
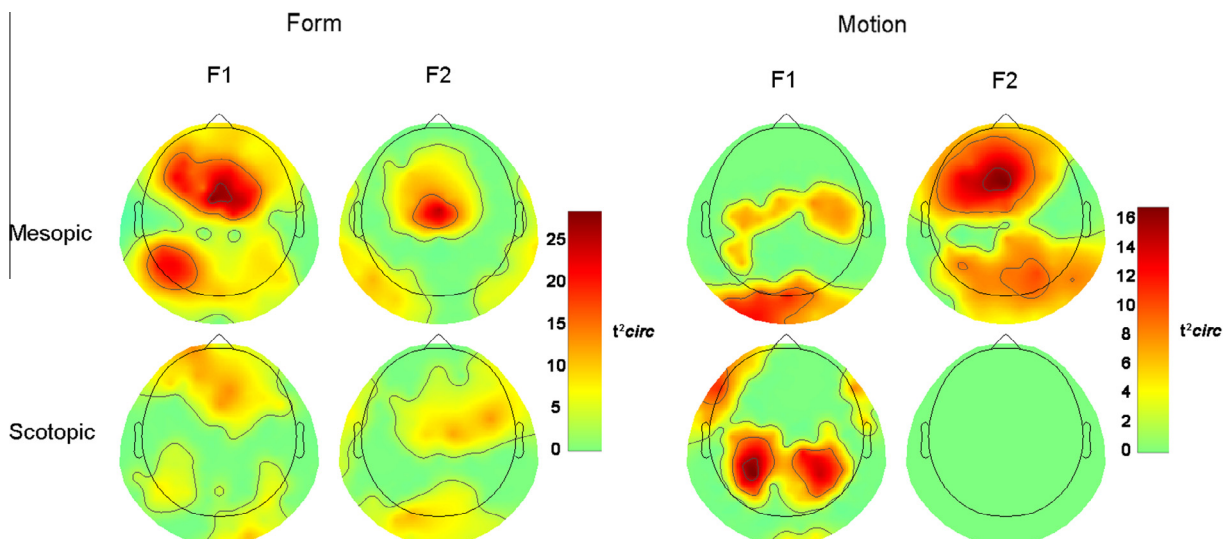

Fig. 4. T^2_{circ} topographic plots of global form and motion activation. F1 activation relates to responses to the global structure of the stimulus whilst F2 activation relates to local changes in the stimulus display.
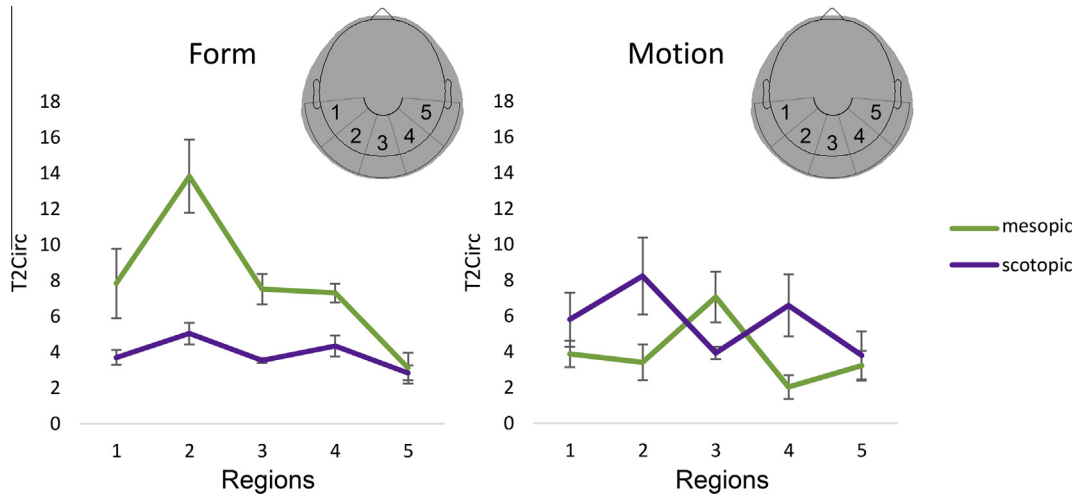
Fig. 5. Mean mesopic and scotopic T^2_{circ} values for the form and motion tests across five regions of the scalp. Error bars represent the standard error of the mean.

A repeated measures test x light x region ANOVA found a main effect of test ($F(1,7) = 5.732$, $p = 0.048$), light ($F(1,7) = 55.187$, $p < 0.001$) and region ($F(4,28) = 14.075$, $p < 0.001$). There were also significant interactions between test * region ($F(4,28) = 4.404$, $p = 0.007$), light * region ($F(4,28) = 6.029$, $p = 0.001$) and test * light * region ($F(4,28) = 3.571$, $p = 0.018$), indicating that responses to the two tests differed across light conditions and across the cortical surface.

3.3. Contrast sensitivity functions

Group average CSF plots are shown in Fig. 6. The qCSF method (Lesmes et al., 2010) calculated four parameters of the CSF and these were used to plot the function. The solid line represents the group average contrast sensitivity as calculated for each light level. The shaded region around the line represents the 95% confidence interval for the group average. Contrast sensitivity reduced
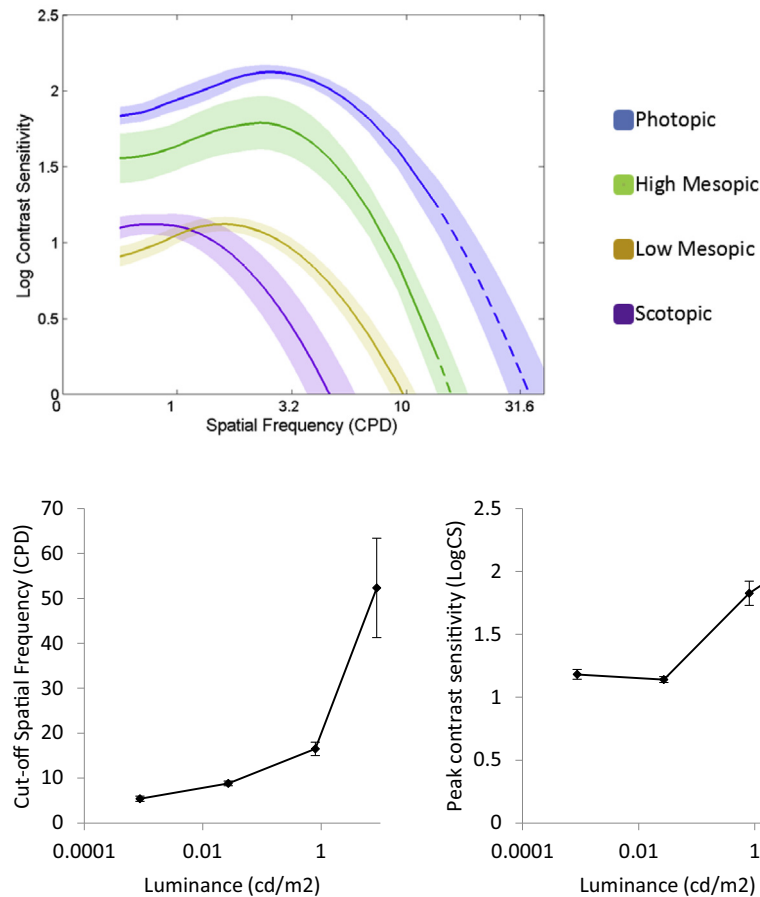

Fig. 6. CSF for each light level (top) and cut-off SF and peak CS across light condition (bottom), error bars represent the standard error of the mean. Solid lines of the CSF represent the group average, shaded regions represent the 95% confidence interval around the mean. In the two brightest conditions participants could detect the highest spatial frequency available from the display, portions of fitted CSF curves above this frequency (13.75 CPD) are shown by the dotted lines.
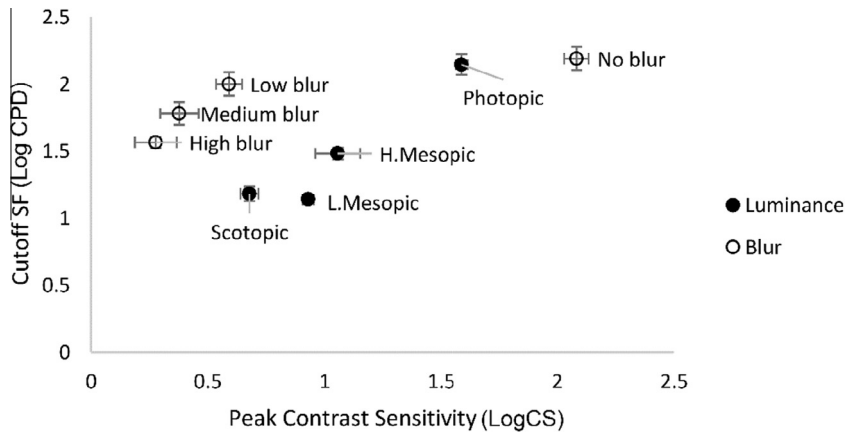
Fig. 7. Comparison of CSF results previously achieved with varying blur (Burton et al., 2015) compared to CSF results achieved here with varying luminance. Mean cut-off SF is plotted against mean peak CS. Error bars represent the standard error of the mean.

as a function of luminance. Decreased light levels led to participants having a lower visual acuity, as demonstrated by the reduced cut-off spatial frequency (cut-off SF), the estimated cycles-per-degree (CPD) at which sensitivity is 0, and reduced peak contrast sensitivity (peak CS).

Within the photopic and high mesopic condition there were ceiling effects in all participants due to limitations of the display monitor and testing distance. The maximum spatial frequency that could be displayed was 1.14 Log CPD = 13.75 CPD, an acuity which all participants exceeded at photopic and high mesopic levels. Data above this value are represented with a dotted line and were derived from the fitted CSF.

Two variables were calculated from the CSF – the cut-off spatial frequency (cut-off SF) and the peak contrast sensitivity (peak CS). Fig. 6 shows the mean cut-off SF and peak CS across participants for each light level. Reducing luminance significantly reduced the cut-off SF ($F(1.025, 16.392) = 13.37$, $p < 0.001$) and peak CS ($F(3, 48) = 87.079$, $p < 0.001$).

As expected, the light level manipulations affected basic spatial sensitivity as indexed by the CSF (Fig. 6), which could potentially contribute to effects on global form and motion perception. To test the extent to which reductions in global form and motion thresholds under low light could be explained by reductions in contrast sensitivity and acuity alone, results were compared to data col-
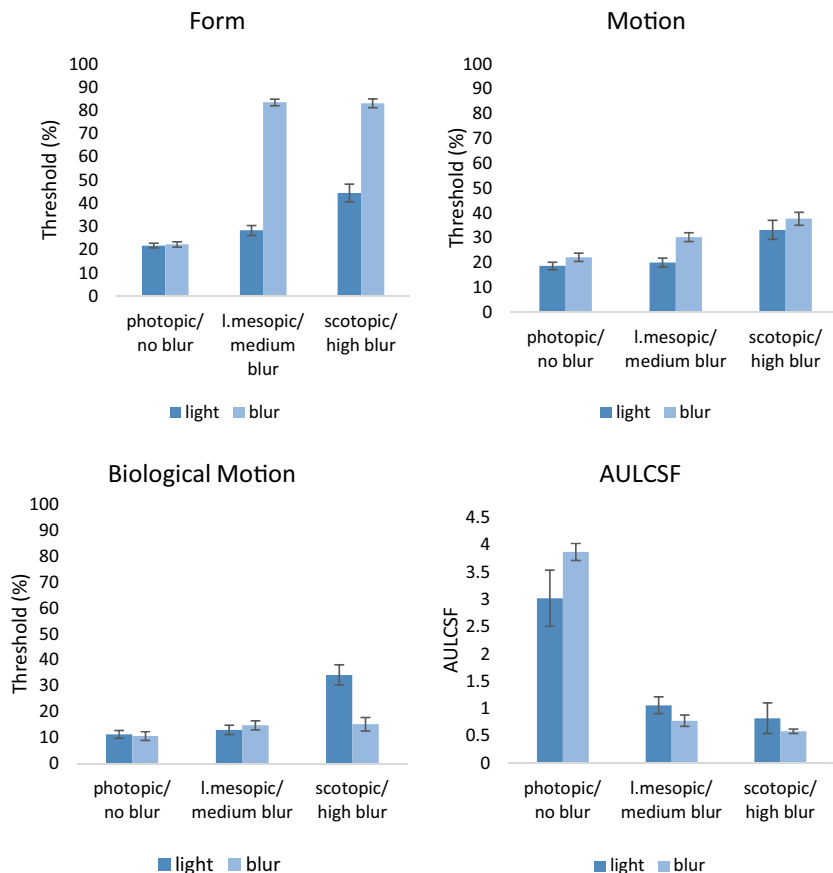

Fig. 8. Comparison of form, motion and biological motion thresholds attained in the photopic, low mesopic and scotopic conditions to those attained with no blur, medium blur and high blur AULCSF results were matched and are shown.

lected previously in 20 typically sighted participants with simulated low vision (Burton et al., 2015). These participants completed the same coherent form and motion tests used here, viewed through a diffuser acting as a low pass filter at different separations from the screen which introduced different levels of blur. All testing was carried out under photopic conditions with an average screen luminance of 30.5 cd/m^2. The form and motion stimulus properties and test setup used in the blur experiment were identical to those described here. This luminance was higher than the photopic luminance used here, since the latter was set to a low level to be comfortable in future use with patients with cone dysfunction.

Fig. 7 shows the effects on the CSF of the four blur conditions and the four different luminance levels employed in the present experiment. The blur effects approximately span the reductions of cut-off SF and peak CS produced by luminance reduction, although blur introduces greater reduction of contrast sensitivity and somewhat less reduction in cut-off SF than the low mesopic and scotopic luminance levels. Blur levels were selected which matched most closely the effects of photopic, low mesopic and scotopic conditions: for these, the area under the log contrast sensitivity function (AULCSF) is comparable, as shown in the lower right panel of Fig. 8.

Fig. 8 shows a comparison of form and motion thresholds under blur and luminance conditions which produced comparable effects on CSFs. The differences in global motion and in biological coherence thresholds are relatively small, whilst for global form thresholds, the blur manipulation produces much stronger effects than the luminance manipulation. These results indicate that the balance of effects produced by low luminance is very different from those predicted on the basis of changes in low-level spatial sensitivity: low luminance has a relatively small effect on form thresholds, and blur a large effect compared to their relative effects on motion thresholds.

Form thresholds were significantly worse under blur than in low light ($F(1,19) = 216.463$, $p < 0.001$). This suggests that form perception under low light is better than would be expected given the reduction in spatial vision. Motion thresholds and biological motion thresholds were not significantly different between blur and luminance conditions (motion: $F(1,19) = 3.746$, $p = 0.068$; biological motion: $F(1,19) = 1.999$, $p = 0.174$). There were also significant interactions between the blur/light condition and the three levels tested for form and biological motion results (form: $F(2,38) = 123.076$, $p < 0.001$; biological motion: $F(2,38) = 10.132$, $p < 0.001$) but not for motion ($F(2,38) = 134.236$, $p = 0.079$). Biological motion results were comparatively worse under scotopic conditions than under blur, whilst form were better.

4. Discussion

The current study aimed to understand how mid- and high-level vision is affected by changes in luminance. Coherent form, motion and biological motion were examined using both behavioural and SSVEP techniques to address how cortical processing of these stimuli varies as luminance decreases.

Coherence thresholds for all three stimuli increased with decreasing luminance. However, global form perception fared worse than either global motion or biological motion perception, indicating that motion perception is relatively less affected by low light. SSVEP measures showed reductions in cortical response (i.e., in our measure of signal-to-noise) from mesopic to scotopic viewing for the form stimulus, paralleling the reduction in behavioural discrimination ability. The transition from mesopic to scotopic conditions also led to some reorganization of topography, particularly for motion responses. These shifts in topography

(Fig. 4) may correspond to changes in cortical visual processing leading to relatively spared motion processing under low light.

Participants' CSF results demonstrated reductions in both contrast sensitivity and spatial acuity as luminance decreased. These results were in line with previous findings on scotopic contrast sensitivity (Barten, 1999). However, the effects on global form, motion and biological motion perception were not uniform, suggesting that spatial limitations of scotopic vision are insufficient in explaining mid-and higher-level visual performance under low light. Comparing the results to data previously collected photopically but with stimuli which were blurred in order to reduce the available spatial information, (Burton et al., 2015), scotopic form perception was less impaired than by blur leading to similar overall reductions in spatial vision. This suggests that the level of sensitivity in low light is greater than expected given the spatial impairments. The reason behind this may be that despite matching the blur and luminance conditions based on AULCSF, blur produced a relatively greater loss of contrast sensitivity than low light. It is therefore possible that form perception is more dependent on contrast than acuity at mid spatial frequencies.

The effect of luminance on global form perception had not been studied previously. On behavioural tests, form perception revealed a greater impairment than global or biological motion. Coherent form perception is processed via region V4 of the extra-striate cortex which receives both parvocellular and magnocellular input (Ferrera, Nealey, & Maunsell, 1994). Parvocellular input is greatly reduced in scotopic conditions (Benedek, Benedek, Kéri, Letoha, & Janáky, 2003; Hassler, 1966) and this loss of input to V4 may be contributing impairments in form perception. This is in contrast to magnocellular input which remains largely intact under low light and could therefore be acting to maintain motion perception. Further work with stimuli specifically designed to isolate magnocellular and parvocellular pathways could provide more insight into their relative contribution to form and motion processing under different light levels.

SSVEP responses to form and motion show distinct topographical organisation. The results from the mesopic condition show midline occipital motion responses vs. lateral form responses. These regions of activation match those found by Wattam-Bell et al. (2010) who used the same stimuli and setup. The different patterns of activation for form and motion support the view that these responses are distinct from one another.

Wattam-Bell et al. (2010) found a similar shift in topography to those observed in our study when comparing adult and infant form and motion SSVEPs. Motion SSVEP responses shifted from a lateral response in infants to a midline response in adults. This was attributed to reduced inhibitory feedback mechanisms in the infant visual cortex (Wattam-Bell, Corbett, & Chelliah, 2013). Wattam-Bell et al. (2013) suggested that midline motion SSVEP responses reflect inhibitory feedback to V1 from extra-striate regions, with V1 inhibition playing less of a role in global form perception. The lack of inhibitory feedback seen in the infant cortex is thought to reflect immaturities in cortical development. However, our similar pattern of results indicates that reduced spatial information input to cortical motion mechanisms may have a similar effect. Further source localisation and the use of neuroimaging methods with greater spatial resolution would be needed to confirm the suggestion of a change in the network contributing to the SSVEP.

Biological motion perception was more impaired scotopically than under blur conditions. This may reflect the importance of precise temporal information in conjunction with form recognition for biological motion perception. The sluggish nature of the rod system reduces the accuracy of temporal information reaching the visual cortex (Conner, 1982; Takeuchi & De Valois, 2000). Reduced accuracy will in turn make it harder to extract structural information, leading to a reduced ability to differentiate scrambled from unscrambled biological motion.

Global motion perception was less impaired than global form under low light. However, we did find overall reductions in global motion sensitivity and SSVEP amplitude in low light. This is in contrast to previous studies which have found, coherent motion perception to be largely unaffected by luminance (Billino et al., 2008; Grossman & Blake, 1999). The differences in results are not explained by the light intensities used as our study found impairments from 0.027 cd/m^2 whilst Billino et al. (2008) did not find impairments in their dimmest condition of 0.018 cd/m^2.

One possible reason for the discrepancy, however, could be the speed of the stimuli. Scotopic conditions have their greatest impact at high temporal frequencies. Takeuchi and De Valois (2000) found velocity discrimination of high temporal frequency drifting sine-wave gratings fell as luminance was decreased. Low temporal frequency discrimination, however, was unaffected. Our study used dots moving at 8.6 deg/s, faster than those tested by both Billino et al. (2008) and Grossman and Blake (1999) and this may explain why performance fell in our study. Indeed, when Billino et al. (2008) tested participants with faster coherent motion (6.6 deg/s and 13.2 deg/s) sensitivity did begin to reduce in low light in line with our findings. In contrast Orban, de Wolf, and Maes (1984) have reported low temporal frequencies to show the greatest impairment in low light relative to intermediate temporal frequencies. Testing at lower speeds than those described here may therefore lead to further reductions in scotopic global motion sensitivity.

Previously, Billino et al. (2008) reported a U-shape effect of luminance on biological motion perception with performance worst in mesopic conditions relative to scotopic and photopic conditions. Our results did not find this pattern. Instead, luminance had a monotonic effect on performance with scotopic light causing the most impairment. Billino et al. (2008) argued that interactions between rods and cones in mesopic conditions can lead to disruptions in spatio-temporal processing of the motion. If this was the case our results should have followed the same pattern. However, our participants showed very little change in biological motion thresholds across the photopic and mesopic light levels. Our results therefore suggest that the cone input seen at these light levels aids biological motion detection and no disruptive interactions between rods and cones were observed. Only at scotopic light levels did biological motion thresholds show a decline in performance. Detection of biological motion stimuli under rod vision is therefore not as efficient as under conditions favouring cones.

5. Conclusion

In conclusion, we found different effects of low light on perceptual sensitivity and cortical responses to coherent form and motion stimuli. These effects were not well explained by basic reductions in spatial vision, but indicate specific effects of low light on extrastriate visual processing. These results provide an initial insight into how patients with retinal dystrophies may perceive global form, motion and biological motion. For example, patients with cone disorders whose rods are unaffected might be expected to show performance similar to our scotopic condition, in which controls relied on rods for vision. This would predict severely impaired global form perception but relatively spared motion perception. However, there is also the possibility that retinal dystrophies present from a young age may lead to different development of the cortical processing that underlies these visual skills. Future work will test this by carrying out these tasks with patient groups.

Acknowledgments

Appendix A. Supplementary data

Supplementary data associated with this article can be found, in the online version, at http://dx.doi.org/10.1016/j.visres.2016.01.008.

References

Atkinson, J., King, J., Braddick, O., Nokes, L., Anker, S., & Braddick, F. (1997). A specific deficit of dorsal stream function in Williams' syndrome. *Neuroreport, 8*(8), 1919–1922.

Atkinson, J., Wattam-Bell, J., Braddick, O., Birtles, D., Barnett, A., & Cowie, D. (2004). Form vs motion coherence sensitivity in infants: The dorsal/ventral developmental debate continues. *Journal of Vision, 4*(8). http://dx.doi.org/10.1167/4.8.32 [32–32].

Bainbridge, J. W., Mehat, M. S., Sundaram, V., Robbie, S. J., Barker, S. E., Ripamonti, C., ... Ali, R. R. (2015). Long-term effect of gene therapy on Leber's congenital amaurosis. *New England Journal of Medicine, 372*(20), 1887–1897.

Barlow, H. B. (1962). Measurements of the quantum efficiency of discrimination in human scotopic vision. *The Journal of Physiology, 160*(1), 169–188.

Barten, P. (1999). Chapter 3: Models for the spatial contrast sensitivity of the eye. *Contrast sensitivity of the human eye and its effects on image quality* (Vol. 72, pp. 44). SPIE Press.

Benedek, G., Benedek, K., Kéri, S., Letoha, T., & Janáky, M. (2003). Human scotopic spatiotemporal sensitivity: A comparison of psychophysical and electrophysiological data. *Documenta Ophthalmologica, 106*(2), 201–207. http://dx.doi.org/10.1023/A:1022548013313.

Benjamini, Y., & Hochberg, Y. (1995). Controlling the false discovery rate: A practical and powerful approach to multiple testing. *Journal of the Royal Statistical Society. Series B (Methodological)*, 289–300.

Billino, J., Bremmer, F., & Gegenfurtner, K. R. (2008). Motion processing at low light levels: Differential effects on the perception of specific motion types. *Journal of Vision, 8*(3) [Retrieved from http://www.journalofvision.org/content/8/3/14.short].

Braddick, O., Atkinson, J., & Wattam-Bell, J. (2003). Normal and anomalous development of visual motion processing: Motion coherence and 'dorsal-stream vulnerability'. *Neuropsychologia* [Retrieved from http://psycnet.apa.org/psycinfo/2003-09334-006].

Braddick, O. J., O'Brien, J.-M., Wattam-Bell, J., Atkinson, J., Hartley, T., & Turner, R. (2001). Brain areas sensitive to coherent visual motion. *Perception, 30*(1), 61–72.

Brainard, D. H. (1997). The psychophysics toolbox. *Spatial Vision, 10*, 433–436.

Burton, E., Wattam-Bell, J., Rubin, G. S., Atkinson, J., Braddick, O., & Nardini, M. (2015). The effect of blur on cortical responses to global form and motion. *Journal of Vision, 15*(15), 1–14.

Cavonius, C. R., & Robbins, D. O. (1973). Relationships between luminance and visual acuity in the rhesus monkey. *The Journal of Physiology, 232*(2), 239–246.

Chaparro, A., & Young, R. S. (1989). Reading with the rod visual system. *Applied Optics, 28*(6), 1110–1114.

Chaparro, A., & Young, R. S. (1993). Reading with rods: The superiority of central vision for rapid reading. *Investigative Ophthalmology & Visual Science, 34*(7), 2341–2347.

Cideciyan, A. V., Aleman, T. S., Boye, S. L., Schwartz, S. B., Kaushal, S., Roman, A. J., & Wilson, J. M. (2008). Human gene therapy for RPE65 isomerase deficiency activates the retinoid cycle of vision but with slow rod kinetics. *Proceedings of the National Academy of Sciences, 105*(39), 15112–15117.

Conner, J. D. (1982). The temporal properties of rod vision. *The Journal of Physiology, 332*(1), 139–155.

Cutting, J. E. (1978). A program to generate synthetic walkers as dynamic point-light displays. *Behavior Research Methods, 10*(1), 91–94.

Duffy, K. R., & Hubel, D. H. (2007). Receptive field properties of neurons in the primary visual cortex under photopic and scotopic lighting conditions. *Vision Research, 47*(19), 2569–2574. http://dx.doi.org/10.1016/j.visres.2007.06.009.

Ellemberg, D., Lewis, T. L., Maurer, D., Brar, S., & Brent, H. P. (2002). Better perception of global motion after monocular than after binocular deprivation. *Vision Research, 42*(2), 169–180.

Ferrera, V. P., Nealey, T. A., & Maunsell, J. H. (1994). Responses in macaque visual area V4 following inactivation of the parvocellular and magnocellular LGN pathways. *The Journal of Neuroscience, 14*(4), 2080–2088.

Gallant, J. L., Shoup, R. E., & Mazer, J. A. (2000). A human extrastriate area functionally homologous to macaque V4. *Neuron, 27*(2), 227–235. http://dx.doi.org/10.1016/S0896-6273(00)00032-5.

Golarai (2009). Differential development of the ventral visual cortex extends through adolescence. *Frontiers in Human Neuroscience*. http://dx.doi.org/10.3389/neuro.09.080.2009.

Grossman, E. D., & Blake, R. (1999). Perception of coherent motion, biological motion and form-from-motion under dim-light conditions. *Vision Research, 39*(22), 3721–3727.

Gunn, A., Cory, E., Atkinson, J., Braddick, O., Wattam-Bell, J., Guzzetta, A., & Cioni, G. (2002). Dorsal and ventral stream sensitivity in normal development and hemiplegia. *Neuroreport, 13*(6), 843–847.

Harvey, B. M., Braddick, O. J., & Cowey, A. (2010). Similar effects of repetitive transcranial magnetic stimulation of MT+ and a dorsomedial extrastriate site including V3A on pattern detection and position discrimination of rotating and

radial motion patterns. *Journal of Vision, 10*(5), 21. http://dx.doi.org/10.1167/10.5.21.

Hassler, P. D. R. (1966). Comparative anatomy of the central visual systems in day- and night-active primates. In R. Hassler & H. Stephan (Eds.), *Evolution of the forebrain* (pp. 419–434). Springer US [Retrieved from http://link.springer.com/chapter/10.1007/978-1-4899-6527-1_40].

Hou, C., Gilmore, R. O., Pettet, M. W., & Norcia, A. M. (2009). Spatio-temporal tuning of coherent motion evoked responses in 4–6 month old infants and adults. *Vision Research, 49*(20), 2509–2517. http://dx.doi.org/10.1016/j.visres.2009.08.007.

Jacobson, S. G., Cideciyan, A. V., Ratnakaram, R., Heon, E., Schwartz, S. B., Roman, A. J., ... Hauswirth, W. W. (2012). Gene therapy for leber congenital amaurosis caused by RPE65 mutations: Safety and efficacy in 15 children and adults followed up to 3 years. *Archives of Ophthalmology, 130*(1), 9–24.

Kellnhofer, P., Ritschel, T., Vangorp, P., Myszkowski, K., & Seidel, H.-P. (2014). Stereo day-for-night: Retargeting disparity for scotopic vision. *ACM Transactions on Applied Perception (TAP), 11*(3), 15.

Kinney, J. A. S. (1958). Comparison of scotopic, mesopic, and photopic spectral sensitivity curves. *JOSA, 48*(3), 185–190.

Kleiner, M., Brainard, D., Pelli, D., Ingling, A., Murray, R., & Broussard, C. (2007). What's new in Psychtoolbox-3. *Perception, 36*(14), 1.

Kogan, C. S., Bertone, A., Cornish, K., Boutet, I., Kaloustian, V. M. D., Andermann, E., ... Chaudhuri, A. (2004). Integrative cortical dysfunction and pervasive motion perception deficit in fragile X syndrome. *Neurology, 63*(9), 1634–1639. http://dx.doi.org/10.1212/01.WNL.0000142987.44035.3B.

Komáromy, A. M., Alexander, J. J., Rowlan, J. S., Garcia, M. M., Chiodo, V. A., Kaya, A., ... Aguirre, G. D. (2010). Gene therapy rescues cone function in congenital achromatopsia. *Human Molecular Genetics, 19*(13), 2581–2593.

Kontsevich, L. L., & Tyler, C. W. (1999). Bayesian adaptive estimation of psychometric slope and threshold. *Vision Research, 39*(16), 2729–2737.

Lesmes, L. A., Lu, Z.-L., Baek, J., & Albright, T. D. (2010). Bayesian adaptive estimation of the contrast sensitivity function: The quick CSF method. *Journal of Vision, 10*(3). http://dx.doi.org/10.1167/10.3.17 [17.1–21].

Lewis, T. L., Ellemberg, D., Maurer, D., Wilkinson, F., Wilson, H. R., Dirks, M., & Brent, H. P. (2002). Sensitivity to global form in glass patterns after early visual deprivation in humans. *Vision Research, 42*(8), 939–948. http://dx.doi.org/10.1016/S0042-6989(02)00041-X.

Livingstone, M. S., & Hubel, D. H. (1994). Stereopsis and positional acuity under dark adaptation. *Vision Research, 34*(6), 799–802.

Mandelbaum, J., & Sloan, L. L. (1947). Peripheral visual acuity: With special reference to scotopic illumination. *American Journal of Ophthalmology, 30*(5), 581–588.

MATLAB. (2012). *Version 2012a*. The MathWorks Inc.

Norcia, A. M., Pei, F., Bonneh, Y., Hou, C., Sampath, V., & Pettet, M. W. (2005). Development of sensitivity to texture and contour information in the human infant. *Journal of Cognitive Neuroscience, 17*(4), 569–579. http://dx.doi.org/10.1162/0898929053467596.

Nygaard, R. W., & Frumkes, T. E. (1985). Frequency dependence in scotopic flicker sensitivity. *Vision Research, 25*(1), 115–127.

Odom, J. V., Bach, M., Brigell, M., Holder, G. E., McCulloch, D. L., & Tormene, A. P. (2010). ISCEV standard for clinical visual evoked potentials (2009 update). *Documenta Ophthalmologica, 120*(1), 111–119.

Orban, G. A., de Wolf, J., & Maes, H. (1984). Factors influencing velocity coding in the human visual system. *Vision Research, 24*(1), 33–39. http://dx.doi.org/10.1016/0042-6989(84)90141-X.

Ostwald, D., Lam, J. M., Li, S., & Kourtzi, Z. (2008). Neural coding of global form in the human visual cortex. *Journal of Neurophysiology, 99*(5), 2456–2469. http://dx.doi.org/10.1152/jn.01307.2007.

Palomares, M., Pettet, M., Vildavski, V., Hou, C., & Norcia, A. (2009). Connecting the dots: How local structure affects global integration in infants. *Journal of Cognitive Neuroscience, 22*(7), 1557–1569. http://dx.doi.org/10.1162/jocn.2009.21323.

Pelli, D. G. (1997). The VideoToolbox software for visual psychophysics: Transforming numbers into movies. *Spatial Vision, 10*(4), 437–442.

Picton, T. W., Bentin, S., Berg, P., Donchin, E., Hillyard, S. A., Johnson, R., Jr., & Rugg, M. D. (2000). Guidelines for using human event-related potentials to study cognition: Recording standards and publication criteria. *Psychophysiology, 37*(2), 127–152.

Rees, G., Friston, K., & Koch, C. (2000). A direct quantitative relationship between the functional properties of human and macaque V5. *Nature Neuroscience, 3*(7), 716–723. http://dx.doi.org/10.1038/76673.

Riggs, L. A. (1965). Visual acuity. In *Vision and visual perception* (pp. 324). New York: Wiley.

Stockman, A., & Sharpe, L. T. (2006). Into the twilight zone: The complexities of mesopic vision and luminous efficiency. *Ophthalmic and Physiological Optics, 26*(3), 225–239. http://dx.doi.org/10.1111/j.1475-1313.2006.00325.x.

Sundaram, V., Wilde, C., Aboshiha, J., Cowing, J., Han, C., Langlo, C. S., ... Michaelides, M. (2014). Retinal structure and function in achromatopsia: Implications for gene therapy. *Ophthalmology, 121*(1), 234–245.

Takeuchi, T., & De Valois, K. K. (2000). Velocity discrimination in scotopic vision. *Vision Research, 40*(15), 2011–2024.

Taylor, N. M., Jakobson, L. S., Maurer, D., & Lewis, T. L. (2009). Differential vulnerability of global motion, global form, and biological motion processing in full-term and preterm children. *Neuropsychologia, 47*(13), 2766–2778.

Teller, D. Y. (2009). Scotopic vision, color vision, and stereopsis in infants. *Current Eye Research, 20*(3), 199–210.

Victor, J. D., & Mast, J. (1991). A new statistic for steady-state evoked potentials. *Electroencephalography and Clinical Neurophysiology, 78*(5), 378–388.

Wattam-Bell, J., Birtles, D., Nyström, P., von Hofsten, C., Rosander, K., Anker, S., & Braddick, O. (2010). Reorganization of global form and motion processing during human visual development. *Current Biology, 20*(5), 411–415.

Wattam-Bell, J., Corbett, F., & Chelliah, V. (2013). Coherence sensitivity of cortical responses to global form. *Perception ECVP Abstract, 42.* 55–55.

Weinstein, J. M., Gilmore, R. O., Shaikh, S. M., Kunselman, A. R., Trescher, W. V., Tashima, L. M., & Fesi, J. D. (2012). Defective motion processing in children with cerebral visual impairment due to periventricular white matter damage. *Developmental Medicine & Child Neurology, 54*(7), e1–e8.

Westheimer, G. (1965). Spatial interaction in the human retina during scotopic vision. *The Journal of Physiology, 181*(4), 881–894.

Wilkinson, F., James, T. W., Wilson, H. R., Gati, J. S., Menon, R. S., & Goodale, M. A. (2000). An fMRI study of the selective activation of human extrastriate form vision areas by radial and concentric gratings. *Current Biology, 10*(22), 1455–1458. http://dx.doi.org/10.1016/S0960-9822(00)00800-9.

Zelinger, L., Cideciyan, A. V., Kohl, S., Schwartz, S. B., Rosenmann, A., Eli, D., ... Sharon, D. (2015). Genetics and disease expression in the CNGA3 form of achromatopsia: Steps on the path to gene therapy. *Ophthalmology, 122*(5), 997–1007.